REPORT 970

THEORETICAL LIFT AND DAMPING IN ROLL AT SUPERSONIC SPEEDS OF THIN SWEPTBACK TAPERED WINGS WITH STREAMWISE TIPS, SUBSONIC LEADING EDGES, AND SUPERSONIC TRAILING EDGES

By Frank S. Malvestuto, Jr., Kenneth Margolis, and Herbert S. Ribner

SUMMARY

On the basis of linearized supersonic-flow theory, generalized equations were derived and calculations made for the lift and damping in roll of a limited series of thin sweptback tapered wings. Results are applicable to wings with streamwise tips and for a range of supersonic speeds for which the wing is wholly contained between the Mach cones springing from the wing apex and from the trailing edge of the root section. A further limitation is that the tip Mach lines may not intersect on the wing.

For the portion of the wing external to the Mach cones springing from the leading edge of the wing tips, the pressure distributions for lift and roll previously obtained for the triangular wing are valid. For the portion of the wing contained within the wing-tip Mach cones a satisfactory approximation to the exact pressure distributions was obtained by application of a point-source-distribution method developed in NACA TN 1382.

A series of design curves are presented which permit rapid estimation of the lift-curve slope C_{L_α} and damping-in-roll derivative C_{l_p} for given values of aspect ratio, taper ratio, Mach number, and leading-edge sweep.

INTRODUCTION

On the basis of linearized supersonic-flow theory the lift-curve slope C_{L_α} and damping-in-roll derivative C_{l_p} of thin triangular wings with large vertex angles were treated in references 1 and 2. In reference 3 stability derivatives including C_{L_α} and C_{l_p} were presented for a series of sweptback wings tapered to a point. The present analysis is an extension of the investigation reported in reference 3 in that, for a similar range of Mach numbers, the derivatives C_{L_α} and C_{l_p} are evaluated for a series of sweptback wings with finite streamwise wing tips. The wings were derived by cutting off the pointed tips of the sweptback wings reported in reference 3 along lines parallel to the free-stream direction. The introduction of the finite wing tip causes an alteration of the pressure distribution over the portion of the wing contained within the Mach cone springing from the leading edge of each wing tip. The wing-tip disturbances are confined to these tip Mach cones and do not affect the remaining portion of the wing.

For the case of a wing at an angle of attack the exact solution for the pressure distribution in the tip region has been reported in reference 4 by the method of superposition of linearized conical flows. This solution (although integrated therein for the tip loss in lift for some cases) does not lend itself readily to the evaluation of the lift-curve slope for families of wings. In the present report the pressure distributions in the tip region for lift, and for rolling as well, are determined to a close approximation by the application of the method used by Evvard in reference 5. The complete-wing pressure distributions are integrated analytically to obtain the lift-curve slope and damping in roll for general families of wings.

The results of the analysis are given in the form of generalized equations for C_{L_α} and C_{l_p} together with a series of design curves from which rapid estimations of C_{L_α} and C_{l_p} can be made for given values of aspect ratio, taper ratio, Mach number, and leading-edge sweep. Some illustrative variations of the derivatives with these parameters are also presented. The derivatives are valid only for a range of supersonic speeds for which the wing is entirely contained between the Mach cones springing from the wing apex and from the trailing edge of the root chord. An added restriction (which, for practical configurations, materially limits the range of Mach numbers for very small aspect ratios only) is that the Mach lines emanating from the wing tips may not intersect on the wing.

SYMBOLS

x, y, z	Cartesian coordinates of an arbitrary point
ξ, η	x-coordinate and y-coordinate of a point source in XY-plane
u_i, v_i, w_i	induced flow velocities along X, Y, and Z body axes (see fig. 2 (a))
u', v', w'	incremental flight velocities along X, Y, and Z stability axes (see fig. 2 (b))
u, v	oblique coordinates in plane of wing the axes of which are parallel to Mach lines $\left(u=\frac{M}{2B}(\xi-B\eta); \ v=\frac{M}{2B}(\xi+B\eta)\right)$
u_W, v_W	oblique coordinates of a particular point on surface of wing (see fig. 13)

V flight speed

α angle of attack (w'/V)

p, q, r angular velocities about X-, Y-, and Z-axes, respectively

M stream Mach number $(V/\text{Speed of sound})$

M' pitching moment

N yawing moment

μ Mach angle

B cotangent of Mach angle $(\sqrt{M^2-1})$

ϵ angle between leading edge and axis of wing symmetry (see fig. 1)

Λ leading-edge sweep $(90°-\epsilon)$

$\theta_0 = \tan \epsilon$

δ angle between trailing edge and axis of symmetry (see fig. 1)

$$m = \frac{\tan \epsilon}{\tan \mu} = \theta_0 B$$

$$n = \frac{\tan \epsilon}{\tan \delta} = 1 - (1-\lambda)\omega$$

$$v = \frac{y}{\theta_0 x}$$

b wing span

c_r wing root chord

c_t wing tip chord

S wing area

λ taper ratio (c_t/c_r)

A aspect ratio $\left(\dfrac{b^2}{S} = \dfrac{2b}{(1+\lambda)c_r}\right)$

ω geometric parameter of wing

$$\left(\frac{2c_r\theta_0}{b} = \frac{4\theta_0}{A(1+\lambda)} = \frac{4m}{AB(1+\lambda)}\right)$$

S_D region of external flow field (see fig. 3)

S_W region of wing (see fig. 3)

σ slope of stream sheet in external flow field measured in planes for which $\eta = \text{Constant}$ (equivalent to symbol λ used by Evvard)

ϕ perturbation velocity potential on upper surface of wing or of stream sheet in external flow field

P local pressure difference between lower and upper surface of airfoil, positive in sense of lift

ρ density of air

C_P pressure coefficient $\left(\dfrac{P}{\frac{1}{2}\rho V^2}\right)$

$$k = \sqrt{1-m^2}$$

$E'(m)$ complete elliptic integral of second kind with modulus k $\left(\displaystyle\int_0^{\pi/2} \sqrt{1-k^2\sin^2 z}\, dz\right)$

$$E''(m) = \frac{1}{E'(m)}$$

$F'(m)$ complete elliptic integral of first kind with modulus k $\left(\displaystyle\int_0^{\pi/2} \dfrac{dz}{\sqrt{1-k^2\sin^2 z}}\right)$

$$I(m) = \frac{2(1-m^2)}{(2-m^2)E'(m) - m^2 F'(m)}$$

L lift

L' rolling moment

C_L lift coefficient $\left(\dfrac{L}{\frac{1}{2}\rho V^2 S}\right)$

C_l rolling-moment coefficient $\left(\dfrac{L'}{\frac{1}{2}\rho V^2 Sb}\right)$

$$C_{L_\alpha} = \left(\frac{\partial C_L}{\partial \alpha}\right)_{\alpha \to 0}$$

$$C_{l_p} = \left(\frac{\partial C_l}{\partial \frac{pb}{2V}}\right)_{\frac{pb}{2V} \to 0}$$

Subscripts:

$0, 1, 2, \ldots$ particular regions of the wing or external flow fields when associated with S_W or S_D

ex, in region of the wing external to the wing-tip Mach cone and within the wing-tip Mach cone, respectively

$( )_\alpha, ( )_p$ when associated with ϕ, P, and C_P indicate the velocity potential, pressure, and pressure coefficient for angle of attack and rolling, respectively

ANALYSIS

SCOPE

The sweptback wings considered are sketched in figure 1. In the following analysis and in the figures the wing plan form with sweptback trailing edge (fig. 1 (a)) will generally be considered and sketched as the typical wing, but the results of the analysis are equally valid for the wing plan form with the sweptforward trailing edge (fig. 1 (b)). The orientation of the wing with respect to a body system of coordinate axes used in the analysis is indicated in figure 2 (a). The surface velocity potentials, the basic pressure distributions, and the stability derivatives are derived with respect to this system. Figure 2(b) shows the wing oriented with respect to the stability-axes system. To the first order in α (the angle of attack), the derivatives C_{L_α} and C_{l_p} have the same value in the stability system as they do in the principal body-axes system (shown dashed in fig. 2 (b)).

The analysis is limited to wings of vanishingly small thickness that have zero camber and are not yawed with respect to the stream direction. The derivatives are valid only for a range of supersonic speeds for which the wings are always contained between the Mach cones springing from the wing apex and from the trailing edge of the root section of the wing. (A wing traveling at speeds for which this condition
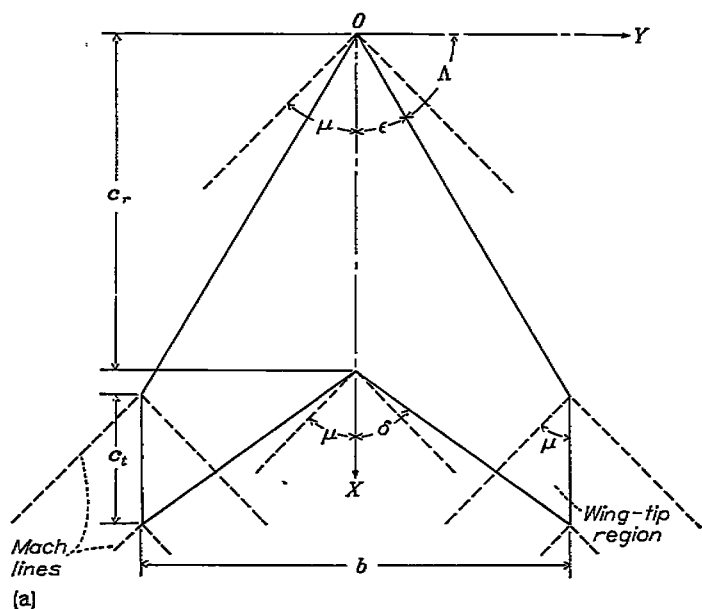
(a) Sweptback trailing edge.

FIGURE 1.—Sweptback wing with streamwise tips and sweptback or sweptforward trailing edges. Note that trailing edge is always inclined at an angle greater than the Mach angle.
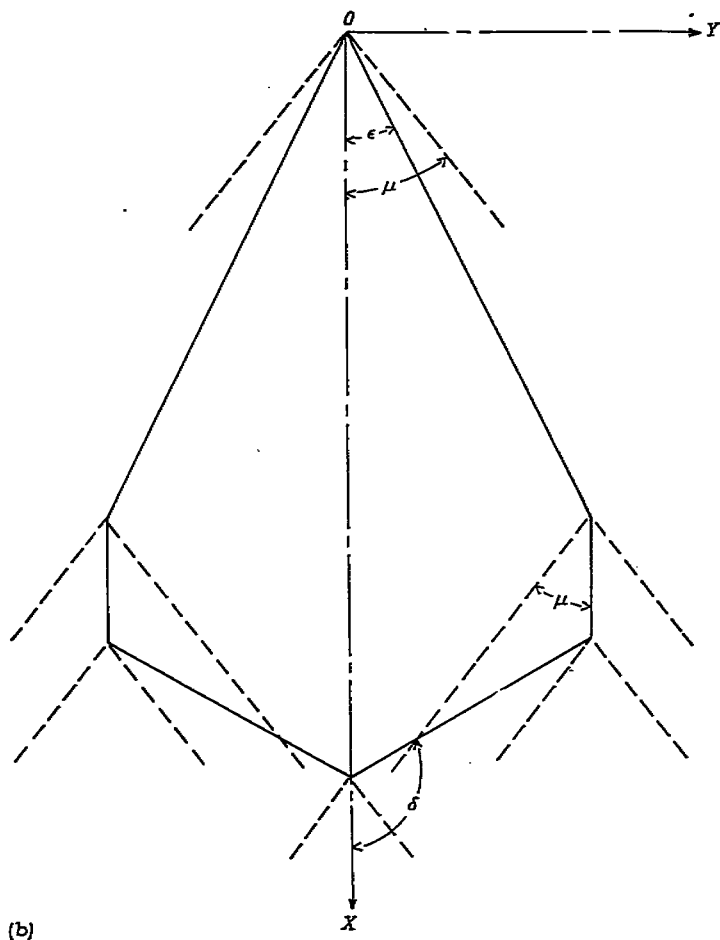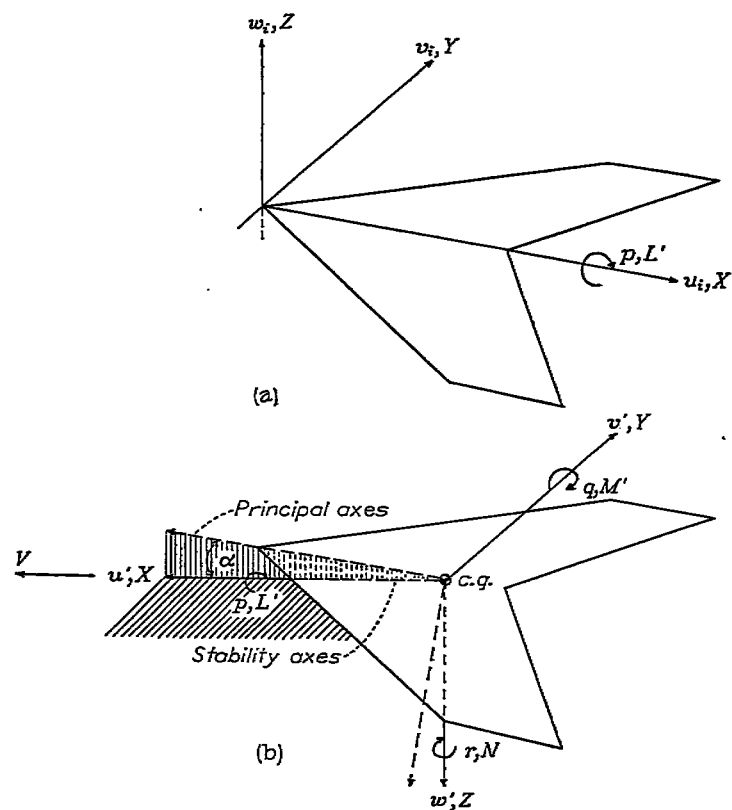
(b) Sweptforward trailing edge.

FIGURE 1.—Concluded.

(a) Notation and body axes used in analysis.
(b) Stability axes. Velocity, force, and moment arrangement in principal-body-axes system is identical to that of stability-axes system. (Principal body axes dashed in for comparison.)

FIGURE 2.—System of axes and associated data.

to the conditions that the stream component normal to the leading edge is subsonic and the component normal to the trailing edge is supersonic.) An added restricton is that the Mach lines emanating from the wing tips may not intersect on the wing. These conditions expressed mathematically as restrictions on B cot Λ are as follows:

For $BA(1+\lambda) \geqq 2$

$$\frac{BA(1+\lambda)}{BA(1+\lambda)+4(1-\lambda)} \leqq B \cot \Lambda \leqq 1$$

and for $BA(1+\lambda)<2$

$$\frac{BA(1+\lambda)}{BA(1+\lambda)+4(1-\lambda)} \leqq B \cot \Lambda \leqq \frac{BA(1+\lambda)}{4-BA(1+\lambda)}$$

BASIC CONSIDERATIONS

The evaluation of the derivatives C_{L_α} and C_{l_p} essentially involves a knowledge of the lifting-pressure distribution over the wing associated with angle of attack for C_{L_α} and with rolling for C_{l_p}. The lifting-pressure coefficients can be determined from the well-known relationships

$$C_P = \frac{P}{\frac{1}{2}\rho V^2} = \frac{2\rho V u_i}{\frac{1}{2}\rho V^2} = \frac{4}{V} u_i$$

or

$$C_P = \frac{4}{V}\frac{\partial}{\partial x}\phi(x,y) \tag{1}$$

is satisfied is now commonly referred to as a wing with subsonic leading edge and supersonic trailing edge. The terms "subsonic leading edge" and "supersonic trailing edge" refer

where $\phi(x,y)$ is the velocity potential on the upper surface of the wing under consideration. The potential $\phi(x,y)$ can be determined by a particular distribution of surface singularities (sources or doublets) which will allow the velocity potential to satisfy the linearized partial-differential equation of the flow and the boundary conditions that are associated with the wing in its prescribed motion.

For the purpose of evaluating the pressure distributions, the wings under consideration can be imagined as consisting of two portions—the segment of the wing external to the Mach cones springing from the leading edge of the wing tips and the segment of the wing within the wing-tip Mach cones (the wing-tip region). The pressure distribution for the wing region external to the wing-tip Mach cones is precisely the same as the pressure distribution for the corresponding section of the triangular wing for the same value of Mach number and leading-edge sweep. For angle of attack and roll the associated pressure distributions for the portion of the wing external to the wing-tip cones have been evaluated in references 1 and 2.

The pressure distribution within the wing-tip Mach cone remains to be determined. For this region the point-source-distribution method of Evvard reported in references 5 and 6 may be applied to the evaluation of an approximate surface velocity potential from which the pressure distribution may be determined. If the considerations of reference 6 are followed, the exact linearized surface velocity potential for a lifting wing is given by (see fig. 3)

$$\phi=\frac{V}{\pi}\int\int_{S_{W\,(0+1+2+3+4)}}\frac{\alpha\,d\xi\,d\eta}{\sqrt{(x-\xi)^2-B^2(y-\eta)^2}}-$$
$$\frac{V}{\pi}\int\int_{S_{D\,(1+2+3+4+5)}}\frac{\sigma\,d\xi\,d\eta}{\sqrt{(x-\xi)^2-B^2(y-\eta)^2}} \qquad (2)$$

The first integral of equation (2) expresses the contribution of the sources distributed over the region of the wing located within the forecone of the point (x,y). The second integral expresses the contribution of the sources over the external flow fields that influence the point (x,y). For the influencing external flow fields the strengths of the source distributions

FIGURE 3.—Sketch of wing regions $S_{W\,(0,\,...\,4)}$ and external flow regions $S_{D\,(1,\,...\,5)}$.

are directly proportional to σ, the component slope of the stream lines parallel to the free-stream direction. It is shown in reference 6 that under certain conditions the contribution to the potential of the source distribution on the wing surface may in part be effectively canceled by the contribution to the potential of the source distribution of the influencing external flow fields. Application of this knowledge to the wing considered herein (fig. 3) gives the following relationships, which are analogous to those obtained for the yawed wing in reference 6:

$$\int\int_{S_{D\,(2+3+4+5)}}\frac{\sigma\,d\xi\,d\eta}{\sqrt{(x-\xi)^2-B^2(y-\eta)^2}}$$
$$=\int\int_{S_{W\,(2+3+4)}}\frac{\alpha\,d\xi\,d\eta}{\sqrt{(x-\xi)^2-B^2(y-\eta)^2}} \qquad (3)$$

and

$$\int\int_{S_{D\,(1+3+4)}}\frac{\sigma\,d\xi\,d\eta}{\sqrt{(x-\xi)^2-B^2(y-\eta)^2}}$$
$$=\int\int_{S_{W\,(1+3)}}\frac{\alpha\,d\xi\,d\eta}{\sqrt{(x-\xi)^2-B^2(y-\eta)^2}} \qquad (4)$$

The substitution of equations (3) and (4) into equation (2) gives the surface velocity potential for the wing-tip region:

$$\phi=\frac{V}{\pi}\int\int_{S_{W,0}}\frac{\alpha\,d\xi\,d\eta}{\sqrt{(x-\xi)^2-B^2(y-\eta)^2}}-$$
$$\frac{V}{\pi}\int\int_{S_{W,3}}\frac{\alpha\,d\xi\,d\eta}{\sqrt{(x-\xi)^2-B^2(y-\eta)^2}}+$$
$$\frac{V}{\pi}\int\int_{S_{D\,(3+4)}}\frac{\sigma\,d\xi\,d\eta}{\sqrt{(x-\xi)^2-B^2(y-\eta)^2}} \qquad (5)$$

It is pointed out in reference 6 that, inasmuch as σ and α have the same sign, the second and third integrals of equation (5) will tend to nullify each other. These integrals will also contribute relatively less than the region $S_{W,0}$ to the potential in the tip region because of the relatively large distance of the fields $S_{W,3}$ and $S_{D\,(3+4)}$ from the tip region. As the areas $S_{W,3}$ and $S_{D\,(3+4)}$ become smaller (Mach lines approaching the leading edge of the wing), their contribution to the potential will tend to become negligible. On the basis of these considerations the second and third integrals of equation (5) were neglected and the surface velocity potential for the wing-tip region may now be expressed approximately by

$$\phi=\frac{V}{\pi}\int\int_{S_{W,0}}\frac{\alpha\,d\xi\,d\eta}{\sqrt{(x-\xi)^2-B^2(y-\eta)^2}} \qquad (6)$$

DERIVATIVE C_{L_α}

The derivative C_{L_α} for the entire wing may be expressed as

$$C_{L_\alpha}=\frac{\partial}{\partial\alpha}(C_{L_{ex}}+C_{L_{in}})=(C_{L_\alpha})_{ex}+(C_{L_\alpha})_{in} \qquad (7)$$

where the subscripts ex and in refer to the part of the wing external to and within the wing-tip Mach cones, respectively.
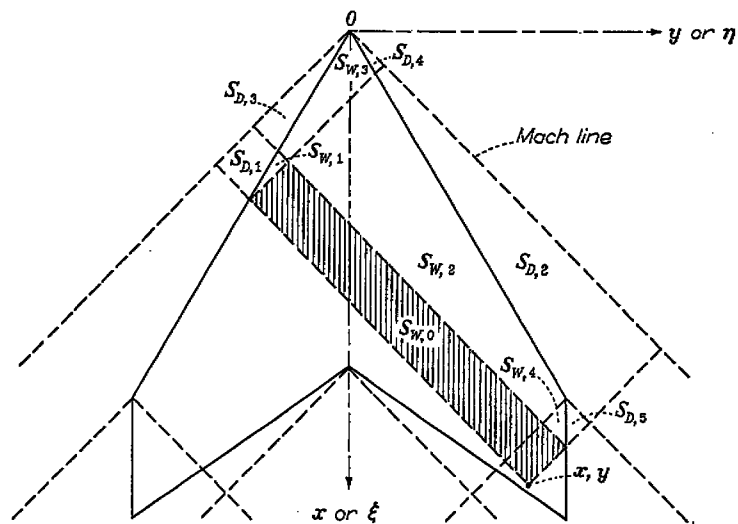
Region of wing external to wing-tip Mach cones.—For the region of the wing external to the tip Mach cone, the pressure distribution is the same as the pressure distribution for the corresponding portion of the triangular wing. This pressure is given in a nondimensional form by the following relationship:

$$(C_{P_{ex}})_\alpha = \frac{(P_{ex})_\alpha}{\frac{1}{2}\rho V^2} = \frac{4\theta_0\alpha}{E'(m)}\frac{1}{\sqrt{1-\nu^2}} \tag{8}$$
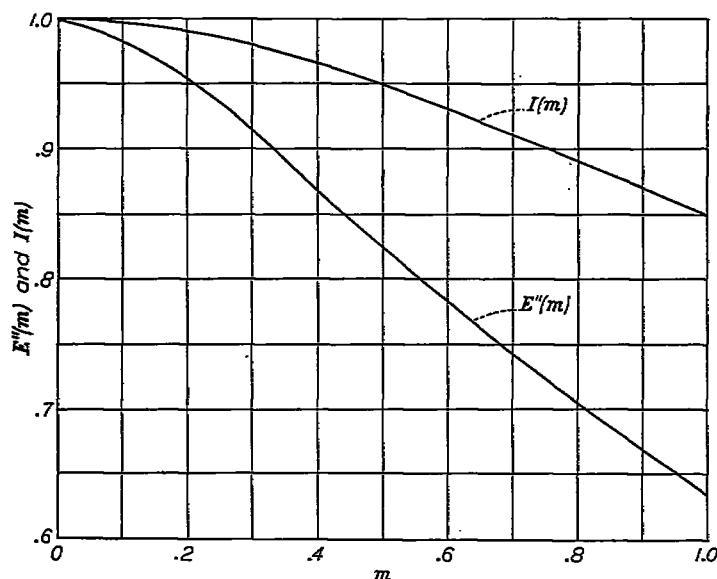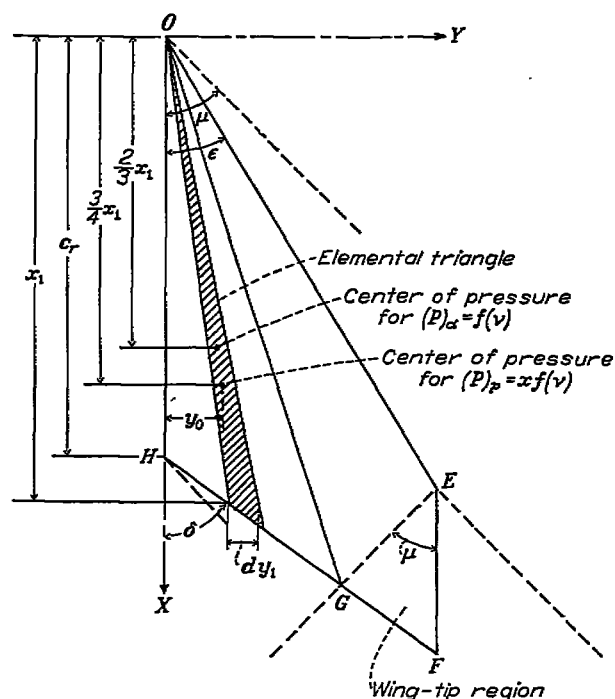

FIGURE 4.—Variation of the elliptic integral factors $E''(m)$ and $I(m)$ with m.

Equation of EG: $x = B\left(\frac{b}{2}-y\right)+\frac{b}{2\theta_0}$

Equation of HF: $x = \frac{y+c_r\tan\delta}{\tan\delta}$

Intersection of EG and HF: $y = \frac{(Bb\theta_0-2c_r\theta_0+b)\tan\delta}{2\theta_0(B\tan\delta+1)}$

FIGURE 5.—Sketch of right panel of sweptback wing showing an elemental triangle and data pertinent to limits of integration.

where ν is proportional to the slope of a ray from the apex of the wing through the point (x,y); that is, $\nu = \frac{y}{\theta_0 x}$. The quantity $E'(m)$ is the complete elliptic integral of the second kind that gives the variation of the pressure with the ratio $\frac{\tan\epsilon}{\tan\mu}$. (See fig. 4.) Integration of the lifting pressure expressed by equation (8) over the wing area external to the tip Mach cones will produce the resultant lift for this portion of the wing. The general conical form $x^n f(\nu)$ noted for the pressure relationship suggests the integration procedure employed in reference 3. Thus the external region of the wing is imagined as composed of an infinite number of elemental triangles (see fig. 5) and the lift is then determined for an elemental triangular area $\left(\frac{1}{2}x_1 dy_1\right)$. The lift coefficient for the external region may then be expressed as follows (for limits of integration, see fig. 5):

$$C_{L_{ex}} = \frac{L}{\frac{1}{2}\rho V^2 S}$$

$$= \frac{2}{S}\left[\int_{\substack{Region\\OHG}}(C_{P_{ex}})_\alpha dS + \int_{\substack{Region\\OGE}}(C_{P_{ex}})_\alpha dS\right]$$

$$= \frac{4c_r^2\theta_0^2\alpha}{SE'(m)}\int_0^{\frac{(1+m)b-2\theta_0c_r}{n(1+m)b+2m\theta_0c_r}}\frac{d\nu}{(1-n\nu)^2\sqrt{1-\nu^2}}+$$

$$\frac{(1+m)^2b^2\alpha}{SE'(m)}\int_{\frac{(1+m)b-2\theta_0c_r}{n(1+m)b+2m\theta_0c_r}}^1\frac{d\nu}{(1+m\nu)^2\sqrt{1-\nu^2}} \tag{9}$$

Region of wing within wing-tip Mach cones.—The lift coefficient $C_{L_{in}}$ for the region of the wing within the wing-tip Mach cone is evaluated by initially determining the surface velocity potential ϕ. For lift the appropriate potential is given by equation (6); that is,

$$(\phi)_\alpha = \frac{V\alpha}{\pi}\int\int_{S_{W,0}}\frac{d\xi\, d\eta}{\sqrt{(x-\xi)^2-B^2(y-\eta)^2}}$$

The evaluation of this equation carried out in appendix A yields

$$(\phi)_\alpha = \frac{2V\alpha}{\pi}\sqrt{\frac{2(By+mx)(b-2y)}{B(1+m)}} \tag{10}$$

The lifting-pressure coefficient is then obtained by the substitution of equation (10) into equation (1):

$$(C_{P_{in}})_\alpha = \frac{4}{V}\frac{\partial}{\partial x}(\phi)_\alpha$$

$$= \frac{8\alpha}{\pi}\sqrt{\frac{\theta_0}{1+B\theta_0}}\sqrt{\frac{\frac{b}{2}-y}{x+\frac{y}{\theta_0}}} \tag{11}$$

In equations (10) and (11) it should be noted that the variables x and y are restricted to the portion of the wing within the wing-tip Mach cones.

Integration of the lifting-pressure coefficient defined by equation (11) will give the resultant lift coefficient for this portion of the wing. The lift coefficient for the wing-tip region may then be expressed as follows (for limits of integration, see fig. 5):

$$C_{L_{in}} = \frac{L}{\frac{1}{2}\rho V^2 S}$$

$$= \frac{2}{S} \int \int_{\substack{Region \\ EGF}} (C_{P_{in}})_\alpha \, dx \, dy$$

$$= \frac{16\alpha}{\pi S} \sqrt{\frac{\theta_0}{1+B\theta_0}} \int_{\frac{b(1+m)-2c_r\theta_0}{2(m+n)}}^{b/2} \int_{B\left(\frac{b}{2}-y\right)+\frac{b}{2\theta_0}}^{\frac{y}{\tan\delta}+c_r} \sqrt{\frac{\theta_0(b-2y)}{2(\theta_0 x+y)}} dx \, dy \tag{12}$$

The result of carrying out the operations indicated in equations (9), (12), and (7) yields the following simplified expression for C_{L_α} of the entire wing in terms of m, $n(>0)$, A, and ω:

$$C_{L_\alpha} = \frac{A}{E'(m)} \left\{ \frac{\omega^2}{(1-n^2)^{3/2}} \left[\sin^{-1}n - \sin^{-1}\frac{(1+m)(n^2-1)+\omega(1+mn)}{\omega(m+n)} \right] + \frac{\sqrt{1+m}}{(1-m)^{3/2}} \cos^{-1}\frac{1+mn+\omega(m-1)}{m+n} + \frac{n\omega^2}{1-n^2} + \right.$$

$$\left. \frac{[\omega n(m-1)+m(n^2-1)]\sqrt{1+m}}{(m+n)(n^2-1)(m-1)} \sqrt{(\omega+n-1)[(1+m)(n+1)+\omega(m-1)]} \right\} +$$

$$\frac{4A}{\pi\sqrt{1+m}} \left\{ \frac{(1+n+\omega)^2}{4(1+n)^{3/2}} \cos^{-1}\frac{(n+\omega)(m-n)+2(1-\omega)+m+n}{(1+n+\omega)(m+n)} - \frac{1}{(1-m)^{3/2}} \cos^{-1}\frac{1+mn+\omega(m-1)}{m+n} + \right.$$

$$\left. \frac{(1+m)(1+n)-\omega(1-m)}{2(m+n)(1-m)(1+n)} \sqrt{(\omega+n-1)[(1+m)(n+1)+\omega(m-1)]} \right\} \tag{13a}$$

When $m=1$, equation (13a) reduces to the following expression:

$$C_{L_\alpha} = \frac{2A}{\pi} \left\{ \frac{\omega^2}{(1-n^2)^{3/2}} \left[\sin^{-1}n - \sin^{-1}\frac{2(n-1)+\omega}{\omega} \right] + \frac{(\omega+n-1)^{3/2}}{(n-1)\sqrt{n+1}} + \frac{n\omega^2}{1-n^2} + \frac{(1+n+\omega)^2}{2\sqrt{2}(1+n)^{3/2}} \cos^{-1}\frac{3-n-\omega}{1+n+\omega} \right\} \tag{13b}$$

<center>DERIVATIVE C_{l_p}</center>

The derivative C_{l_p} is evaluated in a manner similar to that used for C_{L_α}.

Region of wing external to wing-tip Mach cones.—For the region of the wing external to the wing-tip Mach cones, the pressure coefficient is obtained from reference 2 as

$$(C_{P_{ex}})_p = \frac{2pI(m)\theta_0^2}{V}\left(\frac{x\nu}{\sqrt{1-\nu^2}}\right) \tag{14}$$

The corresponding rolling-moment coefficient is expressed by

$$C_{l_{ex}} = \frac{L'}{\frac{1}{2}\rho V^2 S b}$$

$$= \frac{2}{Sb}\left[\int \int_{\substack{Region \\ OHG}} (C_{P_{ex}})_p y \, dy \, dx + \int \int_{\substack{Region \\ OGE}} (C_{P_{ex}})_p y \, dy \, dx \right] \tag{15}$$

The evaluation of equation (15) is simplified by employing the integration procedure used for C_{L_α}. The contribution to the rolling-moment coefficient of each of the elemental triangular areas (see fig. 5) is given by

$$dC_{l_{ex}} = -\frac{y_0}{b} dC_{L_{ex}} \tag{16}$$

where y_0 is the lateral distance of the center of pressure of an elemental triangle from the X-axis of the wing and $dC_{L_{ex}}$ is the lift coefficient of an elemental triangular area. The analysis of reference 3 shows that for a pressure distribution of the form $xf(\nu)$, which is the form of the pressure of equation (14), the lift of an incremental triangle can be expressed as

$$dL_{ex} = \frac{1}{2}\rho V^2 \Delta S_{ex}\, dC_{L_{ex}}$$

$$= \int_{x=0}^{x=x_1} xf(\nu)x\theta_0\, d\nu\, dx$$

$$= \theta_0 f(\nu)\frac{x_1{}^3}{3}\, d\nu$$

$$= \frac{1}{2}\rho V^2\theta_0\frac{(C_{P_{ex}})_p}{x}\frac{x_1{}^3}{3}\, d\nu \qquad (17)$$

where x_1 is the height and ΔS_{ex} the area of an elemental triangle. The quantities x_1 and y_0 given in terms of ν and other parameters may be expressed as follows (see fig. 5):

Region OHG

$$x_1 = \frac{c_r}{1-n\nu}$$

$$y_0 = \frac{3}{4}\frac{c_r}{1-n\nu}\theta_0\nu$$

Region OGE

$$x_1 = \frac{b(1+m)}{2\theta_0(1+m\nu)} \qquad (18)$$

$$y_0 = \frac{3b(1+m)}{8}\frac{\nu}{1+m\nu}$$

Use of equations (16), (17), and (18) leads to the following integral expression for $C_{l_{ex}}$:

$$C_{l_{ex}} = -\frac{c_r{}^4\theta_0{}^4 I(m)p}{SbV}\int_0^{\frac{(1+m)b-2\theta_0 c_r}{n(1+m)b+2m\theta_0 c_r}}\frac{\nu^2 d\nu}{(1-n\nu)^4\sqrt{1-\nu^2}} -$$

$$\frac{b^3(1+m)^4 I(m)p}{16VS}\int_{\frac{(1+m)b-2\theta_0 c_r}{n(1+m)b+2m\theta_0 c_r}}^1 \frac{\nu^2 d\nu}{(1+m\nu)^4\sqrt{1-\nu^2}} \qquad (19)$$

$$C_{l_{in}} = \frac{L'}{\frac{1}{2}\rho V^2 Sb}$$

$$= -\frac{2}{Sb}\int\int_{\substack{Region\\EGF}}(C_{P_{in}})_p y\, dx\, dy$$

$$= \frac{16p\theta_0}{3\pi V Sb(1+m)}\int_{\frac{b(1+m)-2c_r\theta_0}{2(m+n)}}^{b/2}\int_{B\left(\frac{b}{2}-y\right)+\frac{b}{2\theta_0}}^{\frac{y}{\tan\delta}+c_r}\frac{y\left[3\theta_0 x+y(1-2m)-\frac{b}{2}(1+m)\right]\sqrt{\frac{b}{2}-y}}{\sqrt{(\theta_0 x+y)(1+m)}}\, dx\, dy \qquad (23)$$

Region of wing within wing-tip Mach cones.—For the region of the wing within the wing-tip Mach cones, the rolling-moment coefficient is evaluated by employing the approximate surface velocity potential given in equation (6); that is,

$$\phi = \frac{V}{\pi}\int\int_{S_W,0}\frac{\alpha\, d\xi\, d\eta}{\sqrt{(x-\xi)^2-B^2(y-\eta)^2}}$$

The velocity potential given by equation (6) can be expressed so as to apply to the rolling wing by considering the local slope of the airfoil surface with respect to the flow direction. For the thin wings of zero camber considered herein, the slope at any lateral station y is the local angle of attack of the wing and is equal to $p\eta/V$. Substituting $p\eta/V$ for α in equation (6) gives the approximate linearized surface velocity potential for the rolling wing; that is,

$$(\phi)_p = \frac{p}{\pi}\int\int_{S_W,0}\frac{\eta\, d\xi\, d\eta}{\sqrt{(x-\xi)^2-B^2(y-\eta)^2}} \qquad (20)$$

The evaluation of equation (20) carried out in appendix B yields

$$(\phi)_p = \frac{p}{3\pi}\frac{[2yB(2m+1)+bB(m+1)-2mx]\sqrt{2(By+mx)(b-2y)}}{[(1+m)B]^{3/2}} \qquad (21)$$

Differentiation of the potential given in equation (21) yields the pressure distribution for the rolling wing:

$$(C_{P_{in}})_p = \frac{4}{V}\frac{\partial}{\partial x}(\phi)_p$$

$$= -\frac{8p}{V\pi}\left\{\frac{\theta_0\left[3\theta_0 x+y(1-2m)-\frac{b}{2}(1+m)\right]\sqrt{\frac{b}{2}-y}}{3(1+m)\sqrt{(\theta_0 x+y)(1+m)}}\right\} \qquad (22)$$

In equations (21) and (22) the variables x and y are restricted to the portion of the wing within the wing-tip Mach cones. The rolling-moment coefficient for the region of the wing within the wing-tip Mach cones can be expressed as follows (for limits of integration, see fig. 5):

The sum of expressions (19) and (23) is the rolling-moment coefficient for the entire wing. Evaluating the integrals in these

expressions and then differentiating with respect to $\dfrac{pb}{2V}$ give the following derivative C_{l_p} in terms of the parameters m, $n(>0)$, A, and ω:

$$C_{l_p}=\frac{I(m)A}{8}\left\{\frac{\omega^4 n(2n^2+13)}{6(n^2-1)^3}+\frac{\omega^4(4n^2+1)}{2(1-n^2)^{7/2}}\left[\sin^{-1}\frac{(1+m)(n^2-1)+\omega(mn+1)}{\omega(m+n)}-\sin^{-1}n\right]-\frac{(4m^2+1)\sqrt{1+m}}{2(1-m)^{7/2}}\cos^{-1}\frac{\omega(m-1)+mn+1}{m+n}-\right.$$

$$\omega\sqrt{1+m}\frac{(1-\omega+m)\,[n(1+m-\omega)\,(6n^4+10n^2-1)+3(1-9n^2-2n^4)\,(n+mn+m\omega)]+n(2n^2+13)\,(n+mn+m\omega)^2}{6(n^2-1)^3(m+n)^3}$$

$$\sqrt{(\omega+n-1)[(1+m)(1+n)+\omega(m-1)]}+$$

$$\frac{(1-\omega+m)\,[m(1-\omega+m)(1-10m^2-6m^4)+3(1-9m^2-2m^4)(n+mn+m\omega)]-m(2m^2+13)(n+mn+m\omega)^2}{6(m-1)^3(1+m)^{3/2}(n+m)^3}$$

$$\left.\sqrt{(\omega+n-1)\,[(1+m)(1+n)+\omega(m-1)]}\right\}-$$

$$\frac{A}{6\pi(1+m)^{3/2}}\left(\frac{-4(n+1)(1+m-\omega)(1-m)(1+5m)+5\,[(1-n+2m)(n+1-\omega)(1-m)^2+2m(n+1)^2(1+3m)]}{3(1+n)^2(1-m)^2(m+n)^3}\,[m(n+\omega)^2-\right.$$

$$(\omega-1)^2+(n^2-m)]^{3/2}+\frac{5(1+n-\omega)^2(1-n+2m)+4(1+n)\,[(2-3\omega+2m)(1+n)+2\omega^2]}{8(1+n)^3}\left\{\frac{n(n-m)-(2+n)(1-\omega)-m(1+\omega)}{(m+n)^2}\right.$$

$$\left.\sqrt{(\omega+n-1)\,[(1+m)(1+n)+\omega(m-1)]}+\frac{(n+1+\omega)^2}{2(n+1)^{1/2}}\cos^{-1}\frac{m(1+\omega)+(2+n)(1-\omega)-n(n-m)}{(n+1+\omega)(m+n)}\right\}+$$

$$\left.\frac{(1+3m)(4m^2+1)}{(1-m)^3}\left\{\frac{1+mn-\omega(1-m)}{(m+n)^2}\sqrt{(\omega+n-1)\,[(1+m)(1+n)+\omega(m-1)]}-\frac{1}{(1-m)^{1/2}}\cos^{-1}\frac{\omega(m-1)+mn+1}{m+n}\right\}\right) \qquad (24a)$$

For $m=1$, equation (24a) may be expressed in the following manner if the tip region is neglected (see section entitled "Results and Discussion"):

$$C_{l_p}=-\frac{4A\omega}{3\pi}\left(\left\{\frac{4(n-1+\omega)}{105\,\omega(1+n)^3}\,[4(2n^2+10n+23)+3\omega(5\omega-4n-24)]+\right.\right.$$

$$\left.\frac{3\omega^3(4n^2+1)+48(n-1)^3+8(n-1)^2(9-8n)\omega+2\omega^2(n-1)(12n^2-32n+15)}{12\omega(n^2-1)^3}\right\}\sqrt{\frac{n-1+\omega}{1+n}}+$$

$$\left.\frac{\omega^3(1+4n^2)}{8(1-n^2)^{7/2}}\left(\sin^{-1}n-\sin^{-1}\frac{2n-2+\omega}{\omega}\right)-\frac{\omega^3 n(13+2n^2)}{24(n^2-1)^3}\right) \qquad (24b)$$

RESULTS AND DISCUSSION

Formulas have been derived for the evaluation of the derivatives C_{L_α} and C_{l_p} based upon considerations of the linearized supersonic-flow theory. For the wing regions external to the tip Mach cones, the exact linearized pressure distributions for the derivatives were obtained from references 1 and 2. For the portion of the wing within the tip cones, the derivatives were approximately evaluated by applying the method used by Evvard in reference 5.

Although the exact pressure distribution in the tip region is not conical, the approximate pressure distribution given by the present method (equations (11) and (22)) turns out to be conical (in the generalized sense) with respect to the image of the wing tip reflected on the YZ-plane. (See fig. 6.) That is, if x' and y' represent coordinates with respect to the image point, the pressure distribution in the tip region is of the form, for lift

$$P=f_1\left(\frac{y'}{x'}\right)$$

and, for rolling

$$P=f_2\left(\frac{y'}{x'}\right)+xf_3\left(\frac{y'}{x'}\right)$$

In figure 7 the pressure distribution for lift is shown along a chordwise section A–A and a spanwise section B–B, which cut through the wing-tip region. For this region of the wing, a comparison is shown of the approximate pressure determined herein with the exact pressure distribution computed from reference 4. The comparison indicates the satisfactory accuracy of the approximate pressure-distribution relationship. The almost negligible lift in the tip region and the abrupt drop in lift across the inboard Mach line from the wing tip has already been pointed out in reference 4.

The existence of an abrupt drop in lift in crossing the wing-tip Mach line may be readily inferred from Evvard's equation (7a) of reference 7. (Equation (7a) is strictly applicable to a wing with one supersonic leading edge. The leading edges of the wing under discussion, however, are subsonic. The general argument leading to equation (6) herein may be used to justify an approximate application of equation (7a)
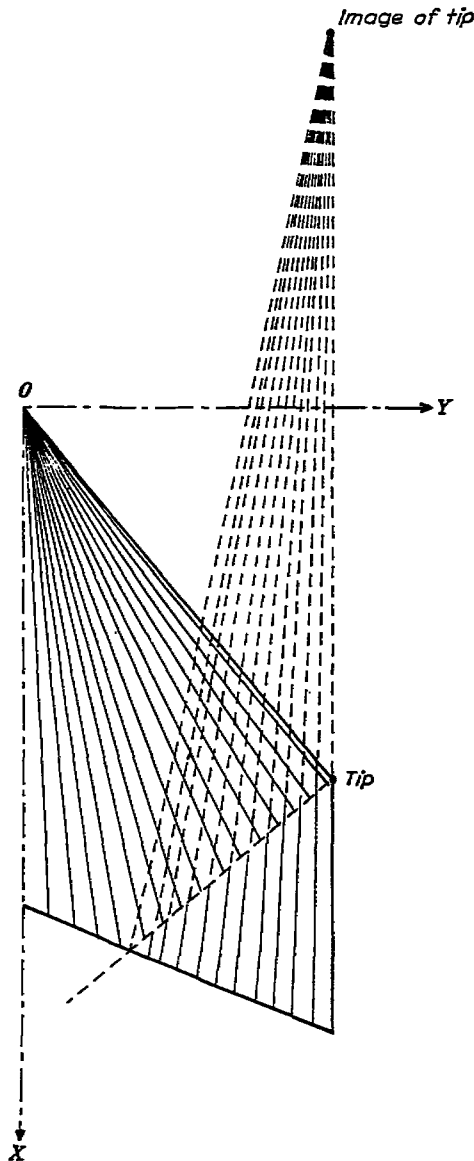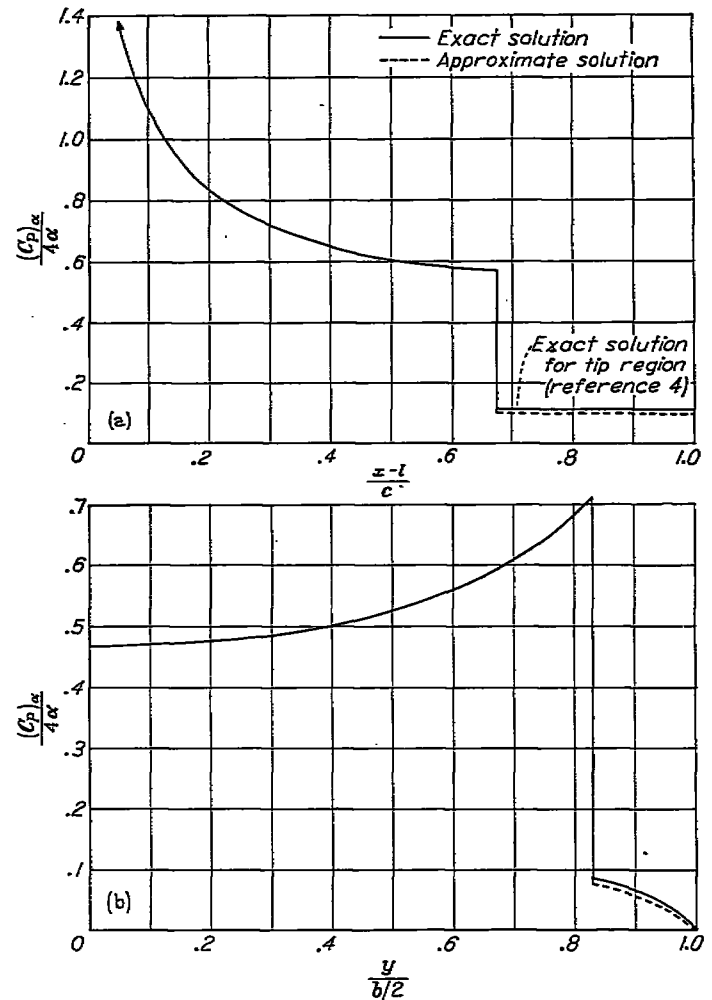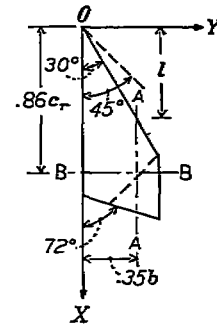
FIGURE 6.—Sketch of right panel of wing indicating conical flow nature of wing-tip region with respect to the image point.

(a) Section A–A; y=Constant.
(b) Section B–B; x=Constant.

FIGURE 7.—Chordwise and spanwise pressure distributions for lift in sectional planes through the wing-tip region.

of reference 7 to the present wing.)   Equation (7a) may be written

$$(C_P)_\alpha = \frac{2\alpha}{B\pi} \int_{ab} \frac{dv - du}{\sqrt{(u_W - u)(v_W - v)}} +$$

$$\frac{4\alpha}{B\pi}\left[1 - \frac{du_2'(v_W)}{dv_W}\right]\sqrt{\frac{v_W - v_1'[u_2(v_W)]}{u_W - u_2'(v_W)}} \qquad (25)$$

This equation gives the pressure coefficient at any point (u_W, v_W), expressed in oblique coordinates. (See fig. of appendix A.)   The second term in equation (25) contains the factor $1 - \dfrac{du_2'(v_W)}{dv_W}$ that involves the slope of the side edge $\dfrac{du_2'(v_W)}{dv_W}$.   Thus any abrupt break in the slope of the side edge gives rise to a discontinuity in the pressure distribution

on crossing the Mach line emanating from the break. In particular, when a portion of the edge is parallel to the stream direction (as is the case for the streamwise wing tip) the value of $\dfrac{du_2'(v_W)}{dv_W}$ is unity.   Hence, the term containing $1 - \dfrac{du_2'(v_W)}{dv_W}$ is zero and the lift is found to drop to a small magnitude on crossing the tip Mach line in the wing-tip region.

Figure 8 shows the chordwise and spanwise pressure distributions for rolling. A similar situation of large finite drop in pressure across the wing-tip Mach line exists for rolling analogous to the lifting case. (See reference 8.) The interesting result obtained is that the rolling pressure is negative in the wing-tip region. This behavior is due to the fact that the sign of the pressure in the wing-tip region is affected only by the angle of attack of the leading edge of the plan form on the opposite side of the roll axis which for positive roll is negative. (See reference 8.)
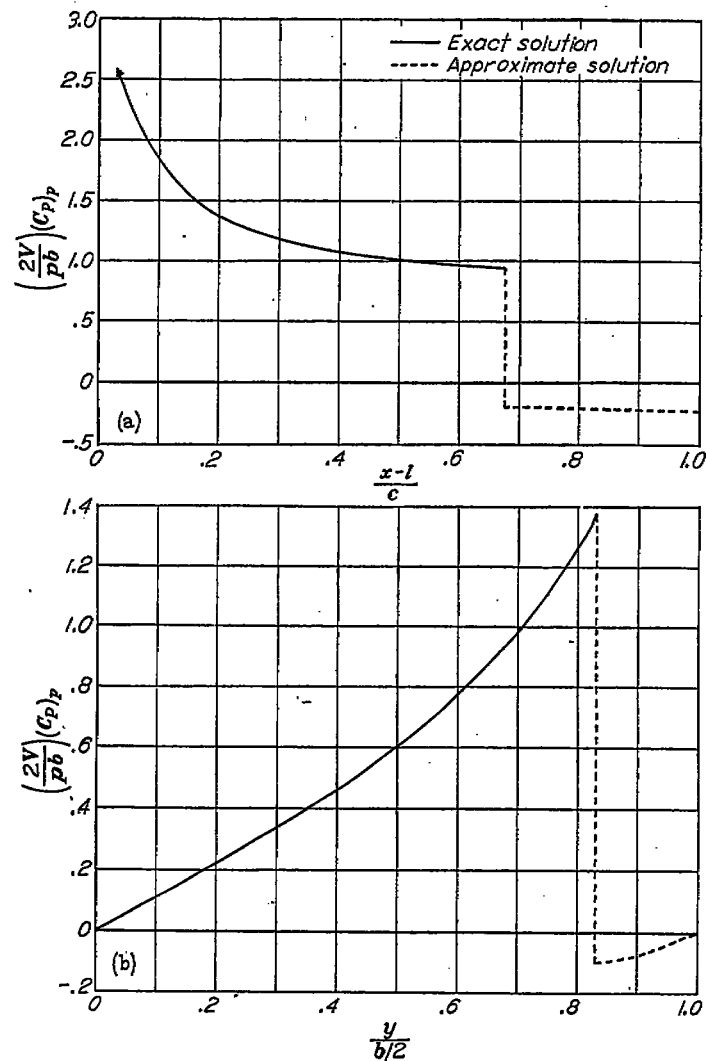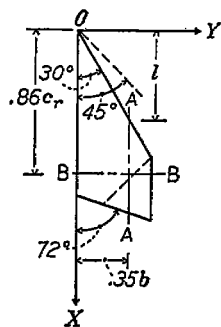
(a) Section A–A; y=Constant.
(b) Section B–B; x=Constant.

FIGURE 8.—Chordwise and spanwise pressure distributions for rolling in sectional planes through the wing-tip region.

The exact solution for the rolling-pressure distribution in the wing-tip region has not at present been determined. In view of the good agreement between the approximate and exact pressure distribution of the lifting case, it is believed that a comparably good agreement should exist for the rolling case. The present approximate method should be adequate for determining the integrated lift and rolling moment, especially since the pressures in the tip region are small. For a practical evaluation of the derivatives, the wing-tip regions may be completely neglected and the resulting error in C_{L_α} and C_{l_p} would be well under 5 percent compared with the values of these derivatives obtained from the method used herein.

A series of generalized design curves are presented in figures 9 and 10. For specified values of aspect ratio, taper ratio, Mach number, and leading-edge sweep, the derivative C_{L_α} may be readily estimated from figure 9 and the derivative C_{l_p} from figure 10. The dashed portions of the curves require special mention. These portions correspond to wing configurations for which the trailing edge is subsonic, in violation of one of the basic assumptions (see section entitled "Scope"), and have the significance of an upper limit below which the true values of the derivatives would lie for the condition of subsonic trailing edge. This circumstance is explained and the limitations on the dashed portions of the curves amplified as follows: In the present calculations the basic conical pressure distribution (except in the tip region) was assumed to persist up to the trailing edge. This procedure is correct for a supersonic trailing edge; but, for a subsonic trailing edge, it neglects the contribution of a region of disturbance due to the edge. This region of disturbance lies between the trailing edge and the Mach lines from the apex of the trailing edge. The neglected subsonic-edge disturbance is in the direction to reduce the lift and the rolling moment. Therefore, the dashed portions of the curves in figures 9 and 10, which correspond to regions of the graph for which the trailing edge is subsonic, overestimate the values of lift or rolling moment. The error is small when the disturbance region is small (sections of dashed curves adjacent to solid sections) and is larger when the disturbance region is large (sections of dashed curves remote from solid sections). Equations for the quantitative evaluations of the trailing-edge disturbance for the lifting case (provided that the Mach lines from the trailing edge of the center section do not intersect the leading edge) are given in reference 4, together with two examples. The major part of the subsonic edge correction is given by equation (55) of that reference. The application of this correction to the design charts for C_{L_α} presented herein affects only a small portion of the dashed sections of the curves immediately adjacent to the solid sections and results in unimportant changes to the values of C_{L_α}.

Specific variations of the derivatives C_{L_α} and C_{l_p} with each of the parameters—aspect ratio, taper ratio, Mach number, and leading-edge sweep—are presented in figures 11 and 12, respectively.
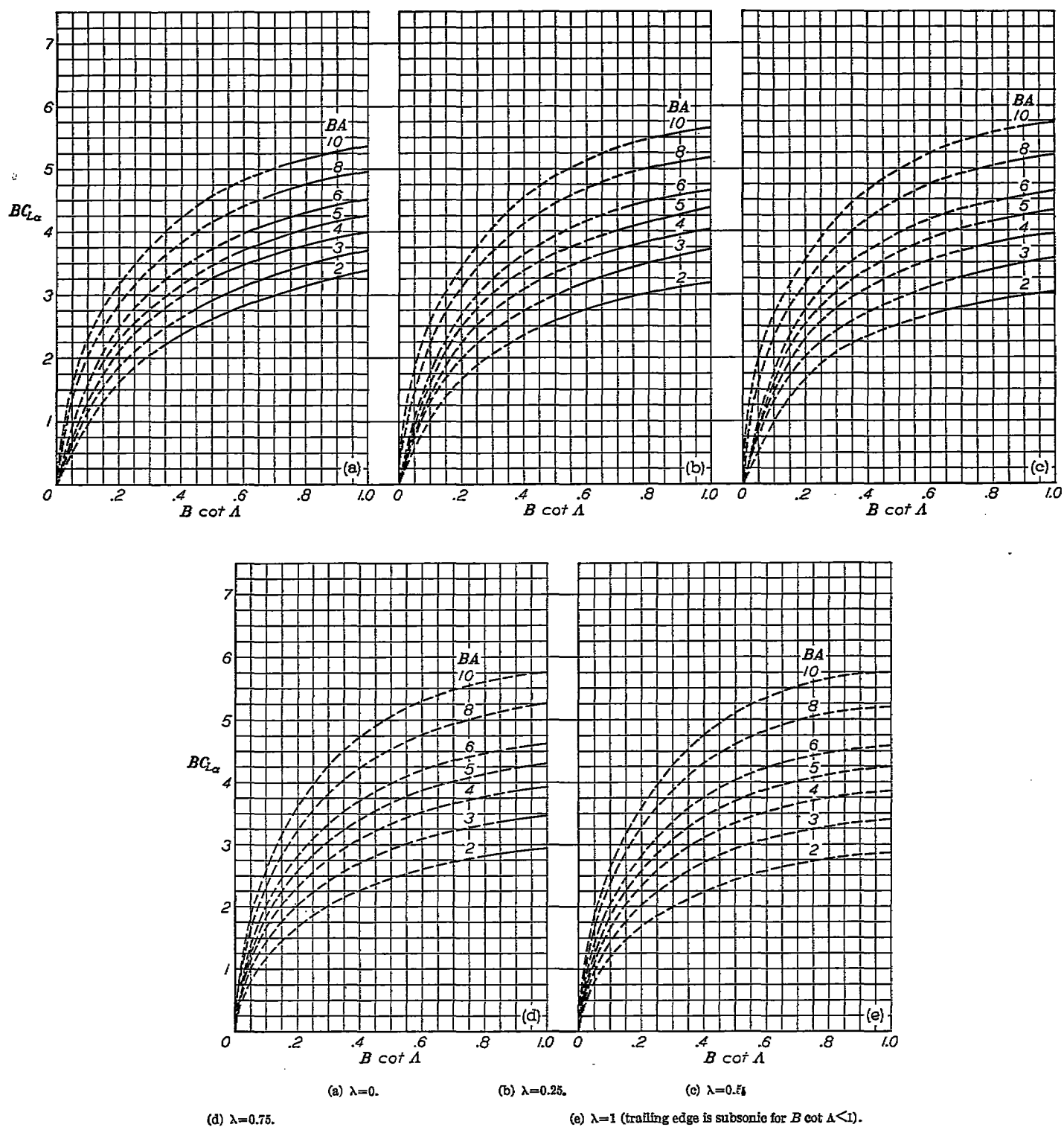
(a) $\lambda=0$. (b) $\lambda=0.25$. (c) $\lambda=0.5$

(d) $\lambda=0.75$. (e) $\lambda=1$ (trailing edge is subsonic for $B \cot \Lambda < 1$).

FIGURE 9.—Variation of BC_{L_α} with $B \cot \Lambda$ for various values of BA and taper ratios. Dashed portions of curves refer to wings with subsonic trailing edges and have limited significance.
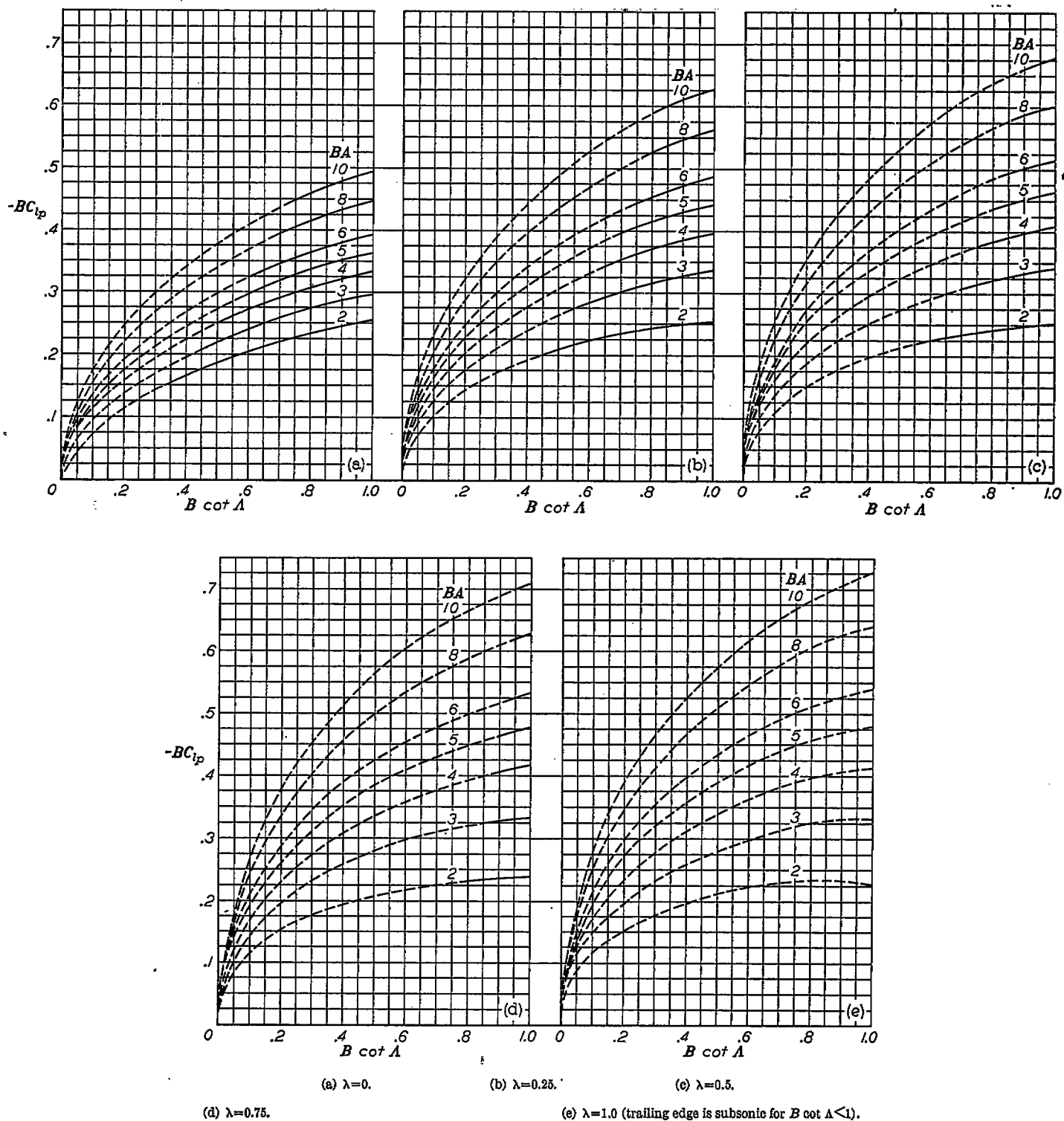
(a) $\lambda=0$.   (b) $\lambda=0.25$.   (c) $\lambda=0.5$.

(d) $\lambda=0.75$.   (e) $\lambda=1.0$ (trailing edge is subsonic for B cot $\Lambda<1$).

FIGURE 10.—Variation of $-BC_{l_p}$ with B cot Λ for various values of BA and taper ratios. Dashed portions of curves refer to wings with subsonic trailing edges and have limited significance.
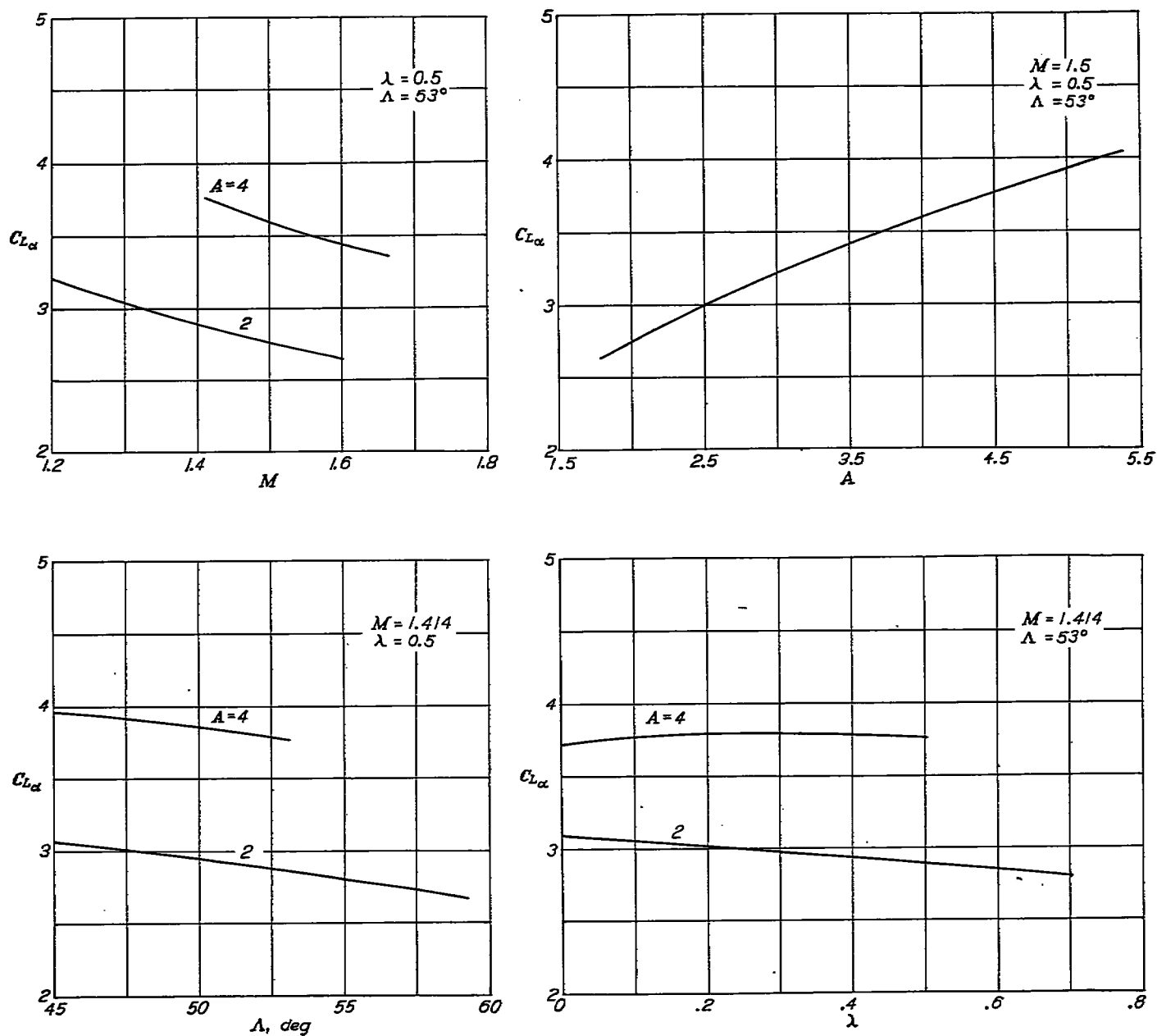
FIGURE 11.—Some illustrative variations of lift-curve slope C_{L_α} with Mach number, aspect ratio, sweepback, and taper ratio.
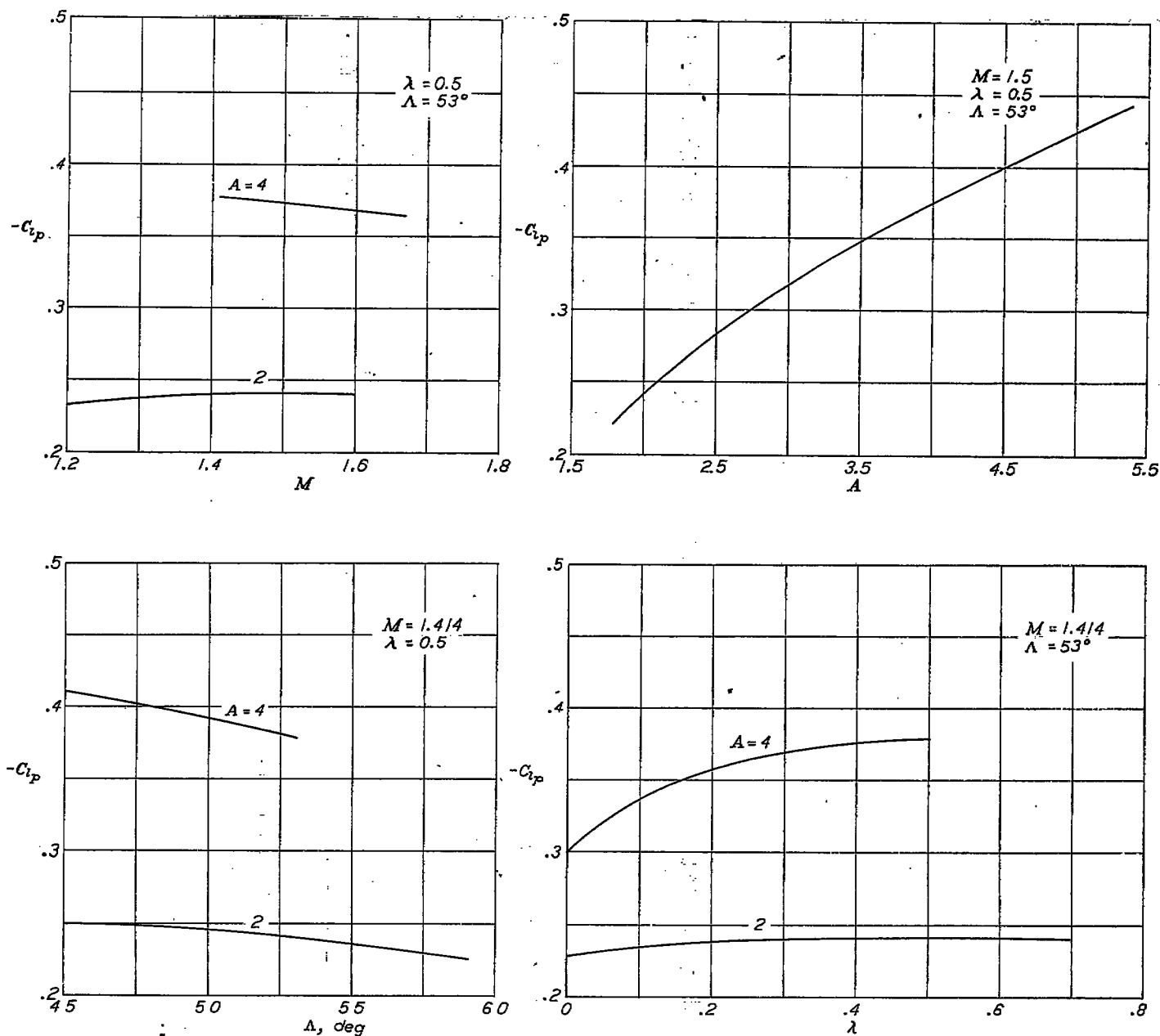
FIGURE 12.—Some illustrative variations of damping-in-roll derivative C_{l_p} with Mach number, aspect ratio, sweepback, and taper ratio.

CONCLUDING REMARKS

Based upon the concepts of linearized supersonic-flow theory, the lift-curve slope C_{L_α} and damping-in-roll derivative C_{l_p} have been evaluated for a limited series of sweptback wings (with streamwise tips) of arbitrary taper and sweep.

The investigation was limited to a range of Mach numbers for which the wing is completely enclosed between the Mach cones springing from the wing apex and from the trailing edge of the root chord of the wing. An added restriction is that the Mach lines from the wing tips may not intersect on the wing.

The results of the analysis are presented in the form of generalized design curves for rapid estimation of the derivatives. Some illustrative variations of the derivatives with aspect ratio, taper ratio, Mach number, and leading-edge sweep are also presented.

LANGLEY AERONAUTICAL LABORATORY,
NATIONAL ADVISORY COMMITTEE FOR AERONAUTICS,
LANGLEY FIELD, VA., *February 15, 1949.*

APPENDIX A

EVALUATION OF POTENTIAL FUNCTION FOR LIFT

The integral expression for the potential

$$(\phi)_\alpha = \frac{V\alpha}{\pi} \int\int_{S_{W,0}} \frac{d\xi\, d\eta}{\sqrt{(x-\xi)^2 - B^2(y-\eta)^2}} \qquad (A1)$$

is easily evaluated by use of an oblique u,v coordinate system, the axes of which lie parallel to the Mach waves. (See reference 5.) The transformation equations are

$$\left.\begin{aligned}
u &= \frac{M}{2B}(\xi - B\eta) \\[4pt]
v &= \frac{M}{2B}(\xi + B\eta) \\[4pt]
\xi &= \frac{B}{M}(v+u) \\[4pt]
\eta &= \frac{1}{M}(v-u)
\end{aligned}\right\} \qquad (A2)$$

When the appropriate substitutions and simplification are performed, equation (A1) becomes

$$(\phi)_\alpha = \frac{V\alpha}{\pi M} \int\int_{S_{W,0}} \frac{du\, dv}{\sqrt{(u_W-u)(v_W-v)}} \qquad (A3)$$

where u_W and v_W are the coordinates of the field point and are related to the x,y system as follows:

$$\left.\begin{aligned}
u_W &= \frac{M}{2B}(x - By) \\[4pt]
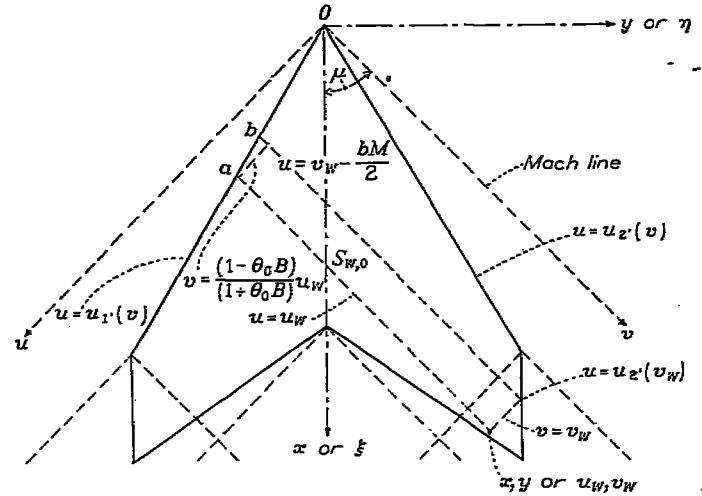v_W &= \frac{M}{2B}(x + By)
\end{aligned}\right\} \qquad (A4)$$

FIGURE 13.—Sketch of wing showing region of integration (area $S_{W,0}$) for the evaluation of the surface velocity potential for lift and roll.

The limits of integration are readily obtained from figure 13 and the potential function may then be expressed as

$$(\phi)_\alpha = \frac{V\alpha}{\pi M} \int_{v_W - \frac{bM}{2}}^{u_W} \frac{du}{\sqrt{u_W - u}} \int_{\frac{1-m}{1+m} u_W}^{v_W} \frac{dv}{\sqrt{v_W - v}} \qquad (A5)$$

The integration yields

$$(\phi)_\alpha = \frac{4V\alpha}{\pi M} \sqrt{\left(v_W - \frac{1-m}{1+m} u_W\right)\left(u_W - v_W + \frac{bM}{2}\right)} \qquad (A6)$$

When equation (A6) is expressed in terms of x,y coordinates, the formula obtained is

$$(\phi)_\alpha = \frac{2V\alpha}{\pi} \sqrt{\frac{2(By + mx)(b - 2y)}{B(1+m)}} \qquad (A7)$$

and is given as equation (10) in the text.

APPENDIX B

EVALUATION OF POTENTIAL FUNCTION FOR ROLL

The integral expression for the potential

$$(\phi)_p = \frac{p}{\pi} \int \int_{S_{W,0}} \frac{\eta \, d\xi \, d\eta}{\sqrt{(x-\xi)^2 - B^2(y-\eta)^2}}$$
(B1)

may be evaluated by the same method used in appendix A.

Upon substitution of the new variables and simplification, equation (B1) becomes

$$(\phi)_p = \frac{p}{M^2} \int \int_{S_{W,0}} \frac{(v-u) \, du \, dv}{\sqrt{(u_W-u)(v_W-v)}} = \frac{p}{M^2} \int_{\frac{1-m}{1+m}u_W}^{v_W} \left[\int_{v_W - \frac{bM}{2}}^{u_W} \frac{(v-u) \, du}{\sqrt{u_W-u}} \right] \frac{dv}{\sqrt{v_W-v}}$$
(B2)

where the limits of integration are obtained from figure 13.

When the integrations indicated in equation (B2) are performed, the following expression is obtained:

$$(\phi)_p = \frac{4p}{3\pi M^2} \left(v_W - \frac{1+3m}{1+m} u_W + \frac{bM}{2} \right) \sqrt{\left(v_W - \frac{1-m}{1+m} u_W \right) \left(u_W - v_W + \frac{bM}{2} \right)}$$
(B3)

Equation (B3) transformed into x,y coordinates becomes

$$(\phi)_p = \frac{p}{3\pi} \frac{[2yB(2m+1) + bB(m+1) - 2mx]\sqrt{2(By+mx)(b-2y)}}{[(1+m)B]^{3/2}}$$
(B4)

and is given as equation (21) in the text.

REFERENCES

1. Brown, Clinton E.: Theoretical Lift and Drag of Thin Triangular Wings at Supersonic Speeds. NACA Rep. 839, 1946.
2. Brown, Clinton E., and Adams, Mac C.: Damping in Pitch and Roll of Triangular Wings at Supersonic Speeds. NACA Rep. 892, 1948.
3. Malvestuto, Frank S., Jr., and Margolis, Kenneth: Theoretical Stability Derivatives of Thin Sweptback Wings Tapered to a Point with Sweptback or Sweptforward Trailing Edges for a Limited Range of Supersonic Speeds. NACA Rep. 971, 1950.
4. Cohen, Doris: The Theoretical Lift of Flat Swept-Back Wings at Supersonic Speeds. NACA TN 1555, 1948.
5. Evvard, John C.: Distribution of Wave Drag and Lift in the Vicinity of Wing Tips at Supersonic Speeds. NACA TN 1382, 1947.
6. Evvard, John C.: The Effects of Yawing Thin Pointed Wings at Supersonic Speeds. NACA TN 1429, 1947.
7. Evvard, John C.: Theoretical Distribution of Lift on Thin Wings at Supersonic Speeds (An Extension). NACA TN 1585, 1948.
8. Moeckel, W. E., and Evvard, J. C.: Load Distributions Due to Steady Roll and Pitch for Thin Wings at Supersonic Speeds. NACA TN 1689, 1948.